At the time of issue this report has not been published. Any author desiring to quote this paper should refer to it as "A paper of the Meteorological Research Committee (London), M.R.P. No. 1025 by C.E. Wallington and Janet Portnall. A copy is available in the Library of the Meteorological Office."

M.R.P.1025
S.C.II/226
2nd January, 1957

AIR MINISTRY

METEOROLOGICAL RESEARCH COMMITTEE

A numerical study of the wavelength and amplitude of lee waves

by

C.E. Wallington and Janet Portnall (Meteorological Office)

Introduction

In a number of papers Scorer (1949 and 1953) has discussed the occurrence of lee waves in the atmosphere and has shown how the values of possible wavelengths may be calculated for an airstream which can be divided into two or more layers each with constant value of a parameter depending on wind and temperature structure. The calculations become rather lengthy if the number of layers exceeds four and it is not clear how much the criteria for lee waves and their wavelength is dependent upon the rather artificial division of the atmosphere into only a few discrete layers.

It is therefore of interest to calculate the wavelength of lee waves in a manner which is convenient for high speed computing and which includes a more detailed treatment of the wind and temperature structure of any given airstream.

As the temperature and wind at great heights are not normally known it is necessary to make some artificial boundary assumptions at the upper limit of the atmospheric layer considered. Our main object in this investigation is to study the effect of these assumptions on the computed wave flow and to test the general applicability of the method by comparing observed and computed lee wavelengths.

The equation of flow

We shall regard the flow as represented by small stationary disturbance imposed on a steady, horizontally uniform stream. Treating the flow as two-dimensional in a vertical plane, an equation can be formed to determine the pressure disturbance, p, at any point on any streamline. Then assuming that hydrostatic equilibrium is maintained, a differential equation defining the flow pattern can be obtained.

For continuity along a stream tube the horizontal velocity component, u, is related to its undisturbed value, U, by the equation

$$u = U\,(1 + \partial h/\partial P)^{-1} \qquad (1)$$

where P is pressure on the streamline in an undisturbed part of the flow.

The equation of continuity enables the vertical velocity component, w, to be given by the equation

$$\rho g w = -U \cdot \frac{\partial p}{\partial x}\left(1 + \frac{\partial h}{\partial P}\right)^{-1} \qquad (2)$$

where ρ denotes the density,

g denotes acceleration due to gravity,

and x is the horizontal co-ordinate.

From the vertical component of the equation of motion we can derive the equation

$$\frac{\partial z}{\partial P} = -\frac{1}{\rho}\left(1 + \frac{\partial h}{\partial P}\right)\left(g + u\frac{\partial w}{\partial x}\right)^{-1} \qquad (3)$$

z being the height.

The second term in the denominator of the right hand side of this equation represents the vertical acceleration of the air and is very small compared with g. Therefore an approximate form of the equation is

$$\frac{\partial z}{\partial P} = -\frac{1}{\rho g^2}\left(1 + \frac{\partial h}{\partial P}\right)\left(g - u\frac{\partial w}{\partial x}\right) \qquad (4)$$

For adiabatic flow of unsaturated air, scalar multiplication of the vector equation of motion by the velocity vector leads to Bernouilli's equation which may be expressed as

$$\rho g z + \frac{1}{2}\rho(u^2 + w^2) + \frac{\gamma}{\gamma - 1}(P + p) = \rho\psi \qquad (5)$$

γ being the ratio of the specific heat of dry air at constant pressure to that at constant volume and ψ being a function of P only.

Differentiating Eq.(5) with respect to P and introducing the potential temperature, θ, referred to a standard pressure level, P_0, we get

$$\frac{1}{2}\rho\frac{\partial}{\partial P}(u^2 + w^2) + \frac{\gamma}{\gamma - 1}\frac{P + p}{\theta}\frac{\partial \theta}{\partial P} + \frac{u}{g}\left(1 + \frac{\partial h}{\partial P}\right)\frac{\partial w}{\partial x} = \rho\frac{\partial \psi}{\partial P} \qquad (6)$$

Equations (1) and (2) may be used to eliminate u and w from Eq.(6) and, for small disturbances only, terms involving powers of p higher than the first may be neglected. Thus after some manipulation Eq.(6) becomes

$$\frac{\partial^2 h}{\partial P^2} + \frac{2}{U}\frac{\partial U}{\partial P}\frac{\partial p}{\partial P} + \left(\frac{R\theta P_0^{\frac{1-\gamma}{\gamma}}}{g P^{\frac{1}{\gamma}}}\right)\frac{\partial^2 p}{\partial x^2} - \frac{R P_0^{\frac{1-\gamma}{\gamma}}}{P^{\frac{1}{\gamma}} U^2} p\frac{\partial \theta}{\partial P} = 0 \qquad (7)$$

where R is the gas constant.

/Method

Method of computation

In order to seek solutions of Eq.(7) which are sinusoidal in the x direction we substitute p = the real part of $f e^{ikx}$, where f is a function of P only, $i = \sqrt{-1}$, and k is a number to be determined. Eq.(7) may then be written in the form

$$\frac{\partial^2 f}{\partial P^2} + 2C \frac{\partial f}{\partial P} + (B - Ak^2) f = 0 \qquad (8)$$

where A, B and C are functions of P only.

The problem of determining the existence and wavelength of lee waves now becomes one of finding values of k ($= K$, say) which permit solutions of Eq.(8) satisfying appropriate boundary conditions. For numerical integration of the equation it is convenient to deal with its finite difference approximation which, after some rearrangement of terms, may be written

$$f_{p+1} = \left[(n^2 A_p k^2 - n^2 B_p + 2) f_p + (n C_p - 1) f_{p-1}\right](n C_p + 1)^{-1} \qquad (9)$$

where the suffixes refer to pressure levels, n being the pressure interval between successive levels.

The lower boundary condition is taken to be $f = 0$ at the 1000 mb pressure level, but it is difficult to justify a definite assumption for the pressure disturbance at some upper boundary. Therefore we take as the upper boundary conditions a unit pressure disturbance at the 200 mb level and make arbitrary trial assumptions of the value of f at 150 mb. Since we do not, at this stage, define a unit pressure disturbance, these assumptions involve only the ratio of the pressure disturbance at 150 mb to that at 200 mb. We shall denote this ratio by ϕ.

In the present series of computations n was given the constant value of 50 mb and the coefficients A_p, B_p and C_p were calculated for 50 mb pressure intervals centred at 200, 250, 300, ... 950 mb.

For each assumed value of ϕ and for values of k = 0, 0.0625, 0.125, 0.1875 ..... 8.0 nautical miles^{-1}, Eq.(9) was used to compute f at 50 mb steps from 250 mb down to the 1000 mb level. Changes of sign for successively computed values of f at 1000 mb showed where to intensify the search for wave numbers which allowed $f = 0$ at 1000 mb. These wave numbers were then calculated to within 6×10^{-6} n.mi.$^{-1}$. The search for values of K was not extended to wave numbers greater than 8 n.mi.$^{-1}$ since experience and theory suggest that short lee waves are usually of small amplitude.

Having computed values of K and corresponding profiles of f it was desirable to assign realistic magnitudes to the pressure disturbance.

Scorer (1949) has derived an expression for the lee wave flow downwind of an 'idealized' two-dimensional ridge whose height, h, at a horizontal distance x from the crest is given by

$$h = \frac{H b^2}{b^2 + x^2} \qquad (10)$$

where H is the height of the ridge and b is a width parameter. Adapting his method to this study we can determine the flow pattern through lee waves induced by such a ridge. The vertical displacement, ζ_z, of a streamline from

its undisturbed level at height z is given by the equations

$$\xi_z = -H b e^{-Kb} \xi_z \sin Kx$$

$$\xi_z = 2\pi \left(\frac{\rho_0}{\rho_z}\right) f_z \left(\frac{\partial f}{\partial K}\right)_0^{-1} \qquad (11)$$

where the suffix 0 refers to the lower boundary level. Values of the lee wave amplitude factor, ξ_z, have been computed and are discussed in the following section.

Discussion of results

The data chosen for numerical study comprised 19 sets of Leuchars radio-sonde ascents in which Corby (1956) had already detected the effect of pronounced lee waves.

Fig. 1 typifies many of the results obtained. Distributions of ξ with height are shown for four of the assumed upper boundary conditions. The full lines show that with $\phi = 0$ two values of K were obtained; the corresponding wavelengths ($2\pi/K$) are given in the figure. For a wavelength of 5.384 n.mi. the amplitude factor, ξ, attains a maximum of 1.05 n.mi.$^{-1}$ in the middle of the stable layer indicated by the observed temperature profile. The longer wavelength of 11.935 n.mi. appears to be associated with a significant lee wave which has a nodal surface at 610 mb. The remaining three pairs of curves relate to $\phi = 1$, 8, and 16. A feature of the ξ curves and the computed wavelengths is that, for the short wavelength, they change only slightly with the upper boundary variation, whereas the long wave value and its amplitude curve were much more sensitive to the choice of ϕ. Particular attention is called to this feature since most of the computed profiles could be classified into two distinct groups: either they varied quickly with variations of the upper boundary assumption or they appeared to change very slowly through a wide (though not unlimited) range of values of ϕ.

Another feature of the plotted curves is that the compact groups such as the short wavelength group of Fig. 1 usually portray waves whose amplitude factors attain only one or two maxima in the troposphere and, apart from a few exceptions, these waves tend to become small near the tropopause. The broad groups on the other hand are usually associated with amplitude curves which vary much more rapidly with height especially in the upper troposphere.

An example of this faature is illustrated in Fig. 2 which shows two compact groups of curves for wavelengths of 2.4 and 4.8 n.mi. and a broad group comprising a set of longer computed wavelengths. The two short waves are confined to the troposphere and it is encouraging to note that Corby detected a wavelength of 4.8 n.mi. for this particular case. The shorter 2.4 n.mi. wavelength was not apparent in his study but inspection of the topography upwind of Leuchars suggests that if this short wave did exist then its maximum vertical velocity would have been smaller than that of the 4.8 n.mi. wave and may therefore have escaped detection. The presence of the broad group of computed longer waves also requires some explanation, for there is no evidence of their actual existence at Leuchars at 04 GMT on 20 November, 1953.

Since the computed values of K and the amplitude of the calculated waves differ greatly according to the choice of upper boundary conditions, there is no reason to think that these solutions correspond to any real dynamical property of the air-stream. If any waves do exist in this band of wavelength, they are inadequately treated by this method, either because they depend on conditions at higher levels or because of inaccuracies in the method.

/Some

Some computing tests have shown that truncation errors may be appreciable for the amplitude curves which exhibit large values of $\partial^2\xi/\partial p^2$ at high levels, but it is not yet possible to make a general statement on the effect of these errors. Until more exhaustive tests have been carried out we must be wary of attaching undue significance to curves of this type.

Thus the compact groups of ξ curves may be subdivided into two categories according to whether they have large or small values of $\partial^2\xi/\partial p^2$ at high levels. The significance of the first category is doubtful but the compact groups of curves without large curvature at high levels may legitimately be interpreted as real waves whose wavelength and amplitude are almost independent of conditions in the high stratosphere. Of the 19 cases examined 13 yielded curves which could be included in this latter category. The observed and computed wavelengths for these cases are listed below.

Date and time	Observed wavelength (n.mi.)	Computed wavelength (n.mi.)
4/11/53 14 GMT	7.2	7.9
18/11/53 14 GMT	7.2	8.1
20/11/53 14 GMT	4.8	4.8 & 2.4
21/12/53 14 GMT	5.4	7.0
3/1/54 03 GMT	10.0	9.2
3/1/54 14 GMT	10.0	9.7
4/1/54 02 GMT	5.6	5.4

Date and time	Observed wavelength (n.mi.)	Computed wavelength (n.mi.)
11/1/54 14 GMT	3.2	4.1
12/1/54 16 GMT	4.8	6.0
23/1/54 14 GMT	3.0	3.1
11/4/54 14 GMT	4.7	4.2
15/4/54 02 GMT	10.1	12.6
15/4/54 14 GMT	7.8	6.2

Two of the remaining six cases produced compact groups of curves with large values of $\partial^2\xi/\partial p^2$ at high levels while the four other cases revealed no definitely compact groups. The nature of the curves obtained in these four cases may be illustrated by reference to Fig. 3. On this occasion ϕ = 4, 8 and 16 led to a compact group of curves with wavelengths close to 9.7 n.mi. but ϕ = 1 failed to produce a curve in this group; instead of one significant curve we obtained two, both of which vary quickly with changes of ϕ. This illustrates the fact that although we may derive the wavelength of about 9.7 n.mi. by making only an approximate guess at the appropriate value of ϕ, our guess must at least be within some wide range. In the four unsolved cases it appeared that none of the trial values of ϕ was within an appropriate range: the ξ profiles comprised only chaotic sets of curves which could not be analysed into compact groups. It was impractical in these four cases to extend the search for suitable values of ϕ, especially since the high level conditions tended to amplify inaccuracies in the method of computation. These inaccuracies are mainly due to the coarseness of the finite difference interval of 50 mb at high levels. It is intended to reduce this interval in future numerical work.

As a further guide to the realism of the computed amplitude factors a comparison between the vertical motion anomalies of the radio-sondes and the calculated vertical speeds was attempted. Usually it was difficult to assess the values of H and γ applicable to the upwind terrain. Nevertheless,

estimates made showed the computed ζ curves with their mean maxima of 1.6 n.mi.$^{-1}$ at an average level of 780 mb to be reasonably consistent with the general magnitude and distribution of the observed vertical speeds.

In one case it was feasible to analyse the high ground profile in detail sufficiently far upwind of Leuchars to include the most effective topographical features. At 1415 GMT on 21 December, 1953 an airstream, whose temperature and wind structure are shown in Fig. 4, blew from about 290° across the Sidlaws to Leuchars. Upwind of Leuchars the high ground profile could be considered as a synthesis of six "ideal" ridges as far as the Tay valley. For some considerable distance further upwind the topographical features did not appear suitable for setting off lee waves on this occasion. Fig. 4 shows the computed vertical motion field in the lee wave over and downwind of Leuchars. Comparison of the observed and computed vertical motion anomalies of the radio-sonde shows that the computations yield vertical speeds of approximately correct magnitudes. There does appear to be a phase difference between the observed and computed wave but this appears to arise from the two-dimensional treatment of two of the "ideal" ridges; the 290° airstream crossed these two ridges close to their northeastern ends and the associated lee wave amplitudes may not therefore have attained their full two-dimensional values.

Conclusion

Comparison of computed lee-wavelengths with those estimated by Corby from the rate of ascent of the radio-sonde balloon, indicate a reasonable accuracy in the computed wavelengths.

The method of calculation as adopted in the present experiment is likely to be inaccurate for lee-waves which have a significant amplitude in the stratosphere. It is not known whether the failure to determine the wavelength satisfactorily in 4 out of the 19 cases is for this reason.

References

Corby, G.A.	1956	Meteorological Research Papers, Air Ministry, London, No. 985.
Scorer, R.S.	1949	Quart.J.R..Met.Soc., 75, p.41.
	1953	Ibid., 79, p.70.

Appendix

Observed and computed wavelengths

In the table below each line of wavelengths is associated with ξ -curves which have similar characteristics or which fall into compact groups.

Wavelengths are given in nautical miles.

Date and time	Observed wavelength	Computed wavelengths for various values of ϕ				Character of ξ curves
		ϕ = 0	1	4	16	
14 GMT 4/11/53	7.2	7.9	7.9	7.9	7.8	C
		5.7	5.3	4.9	4.7	n
		3.7	-	2.5	1.5	n
		ϕ = 0	1	4	16	
14 GMT 18/11/53	7.2	12.0				
			8.2	8.1	8.1	C
		8.0				
			6.2	3.0	1.4	n
		ϕ = 0	1	8	16	
14 GMT 20/11/53	4.8	10.3	6.1	25.5	24.0	X
		4.8	4.8	4.8	4.8	C
		2.4	2.4	2.4	2.4	C
				2.0	1.4	n
		ϕ = 0	1	4	16	
02 GMT 30/11/53	14.4	11.2	33.2	21.2	20.2	
			7.0	3.4	1.6	n
		ϕ = -4	1	4	8	
14 GMT 21/12/53	5.4	34.2				X
		7.0	7.0	7.0	7.0	C
			5.5	3.3	2.3	n
		ϕ = 0	1	4	16	
03 GMT 3/1/54	10.0		9.4			X
		9.1		9.2	9.2	C
			7.9			X
				3.2	1.4	n
		ϕ = 1	4	8	16	
14 GMT 3/1/54	10.0	11.5				
			9.7	9.6	9.6	C
		9.0				
					1.5	n
		ϕ = 0	1	8	16	
02 GMT 4/1/54	5.6	11.9	10.1	7.9	7.6	X
		5.4	5.4	5.4	5.4	C
		3.5	3.1	1.9	1.4	n
		ϕ = 0	1	8	16	
02 GMT 11/1/54	6.5	8.9	8.4	8.1	8.1	CX
		5.7	5.4	5.3	5.2	CX
		4.9	4.8	4.8	4.8	CX
		3.9	2.9	1.3		n
		ϕ = 0	1	4		
14 GMT 11/1/54	3.2	6.5	6.5	6.5		CX
		4.1	4.1	4.1		C

Date and time	Observed wavelength	Computed wavelengths for various values of ϕ				Character of ξ curves
		ϕ = -16	0	16		
16 GMT 12/1/54	4.8	10.1	16.7	10.9		X
		5.9	6.1	5.9		C
			4.6	1.4		n
		ϕ = 0	1	8	32	
02 GMT 14/1/54	5.6	17.5	11.5	10.1	9.6	X
		8.7	8.0	7.2	7.2	X
		5.4	4.4			n
				1.9	1.0	n
		ϕ = 0	1	4	16	
14 GMT 23/1/54	3.0	11.0	11.1	11.1	11.0	CX
		4.5	4.5	4.5	4.5	CX
		4.0	4.0	4.0	4.0	CX
		3.1	3.1	3.1	3.1	C
		1.3	1.3	1.3	1.2	n
		ϕ = 0	1	4	16	
14 GMT 24/1/54	2.6	6.4	6.4	6.4	6.4	CX
		4.9	4.9	4.9	4.9	CX
		3.1	3.1	3.1	3.1	n
		1.9	1.8	1.5	1.0	n
		ϕ = 0	1	8	32	
02 GMT 21/3/54	4.7	20.4	14.1	11.5	11.5	X
		9.9	9.3	7.6	7.1	
		4.0	3.6	2.1	1.1	n
		ϕ = 0	1	8	16	
14 GMT 11/4/54	4.7			18.7	15.7	
		6.1	5.9	5.5	5.5	CX
		4.2	4.2	4.2	4.2	C
		3.7	3.3	1.9	1.4	n
		ϕ = 0	1	4	16	
15 GMT 14/4/54	13.0	12.0	42.3	13.0	12.7	X
			11.0			
				3.9	1.6	n
		ϕ = 1	8	16	32	
02 GMT 15/4/54	10.1	14.2				
			12.8	12.6	12.6	C
		6.7				
			2.6	1.8	1.3	n
		ϕ = 0	4	16		
14 GMT 15/4/54	7.8	10.0				n
		6.2	6.2	6.2		C
			3.5	1.7		n

Characteristics of ξ -curves - {C = Compact group; X = Accuracy doubtful; n = Almost negligible values}

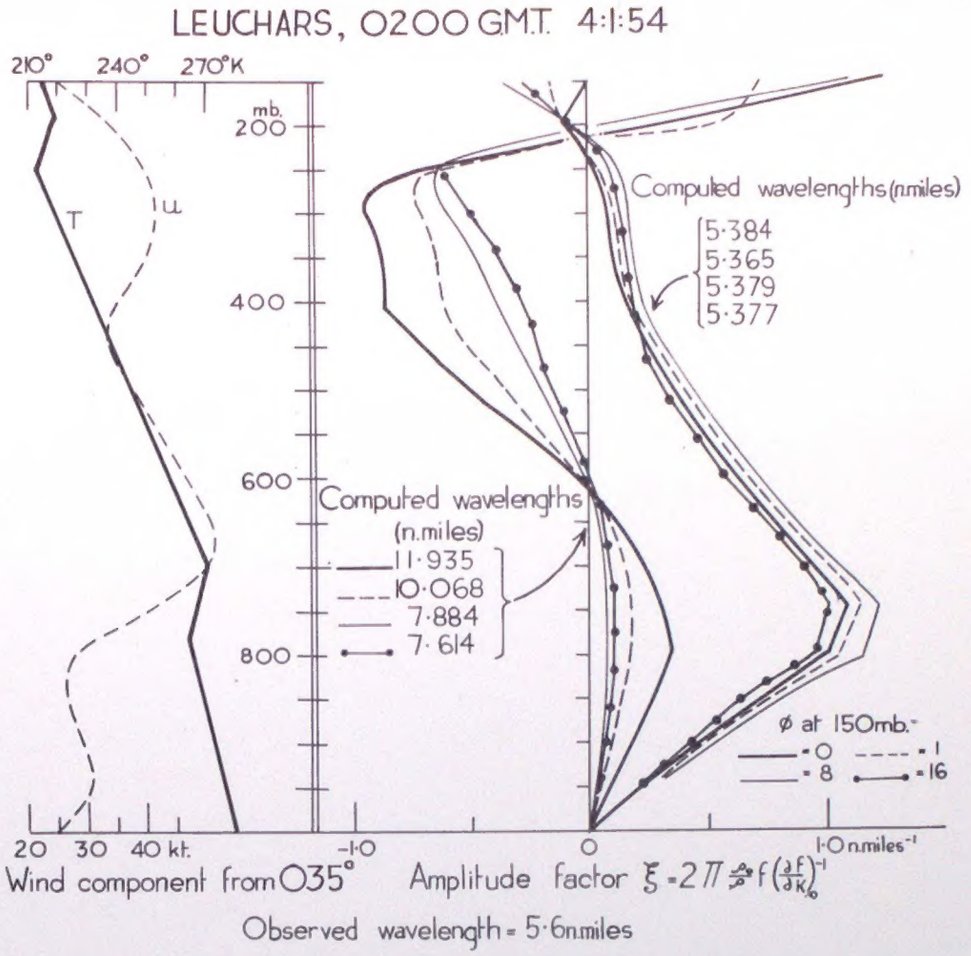

Fig.1

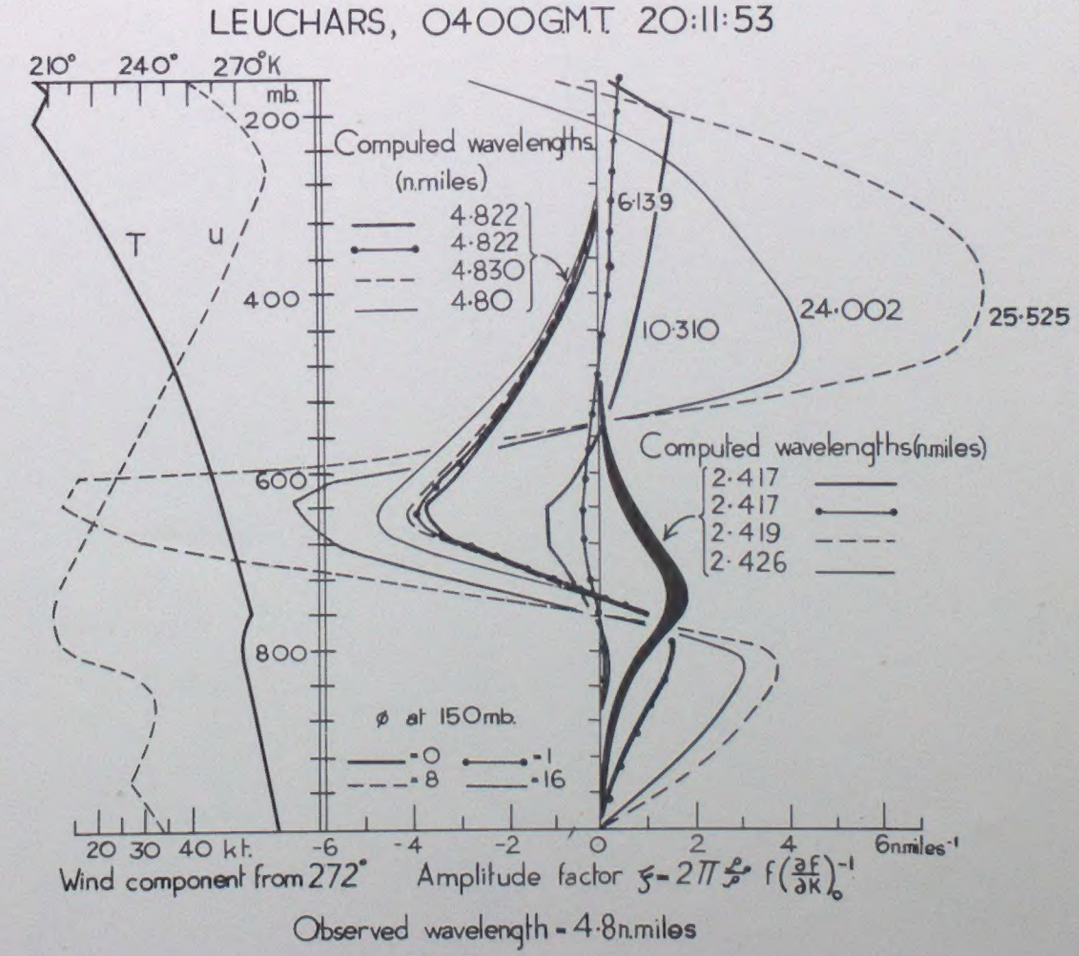

Fig. 2

Figs. 1, 2 and 3. Wind and temperature distribution with height is indicated in the left of the figures. ξ -curves and their associated wavelengths for several values of ø are shown on the right. The observed wavelengths were measured by Corby (1956).

LEUCHARS. 1400 G.M.T. 3:1:54

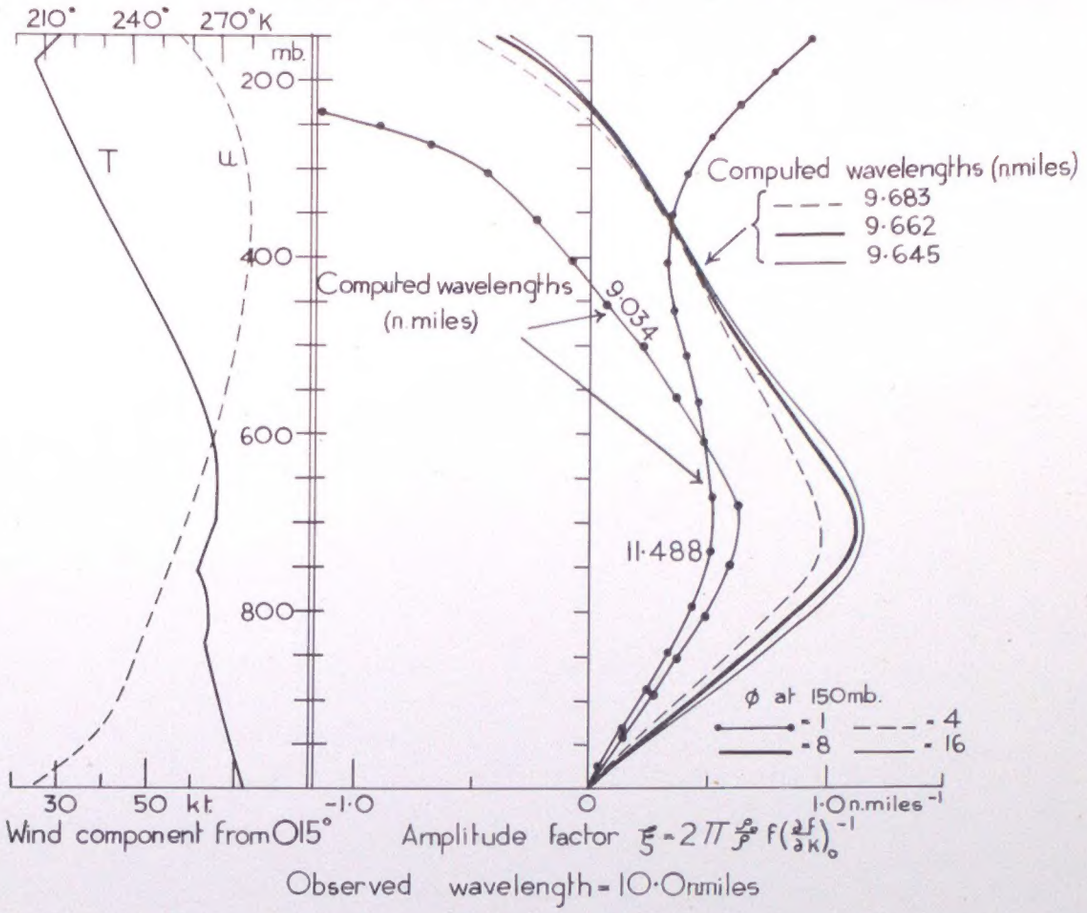

Fig. 3

LEUCHARS, 1415 G.M.T. 21:12:53

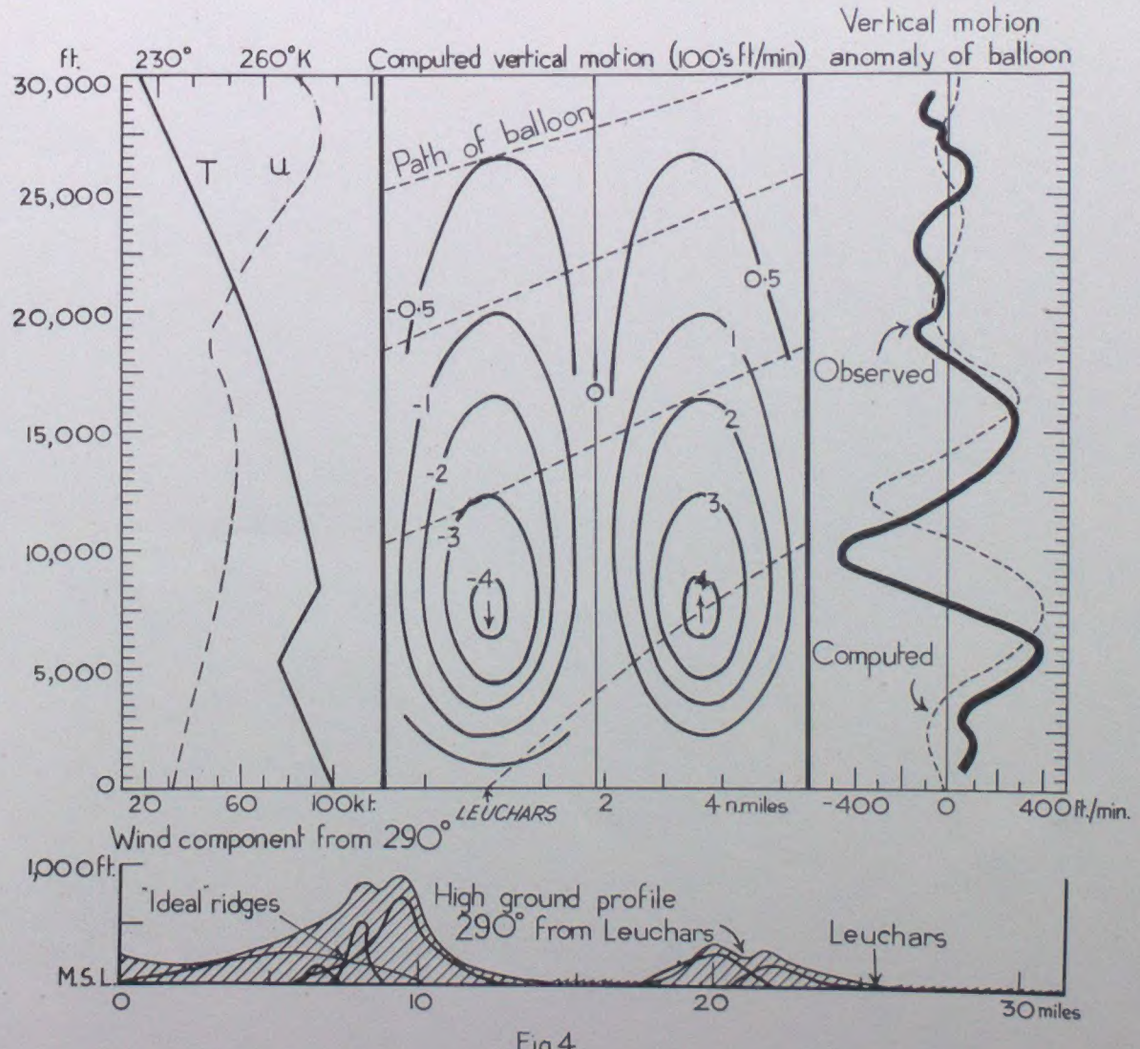

Fig. 4

Fig. 4. The topography upwind of Leuchars may be analysed into the seven 'ideal' ridges shown. The central section of the figure shows the computed vertical motion field over and downwind of Leuchars. The pattern is repeated through each wavelength; the passage of the radio-sonde has therefore been adjusted to save space.